

Spectroscopy and carrier dynamics in CdSe self-assembled quantum dots embedded in $\text{Zn}_x\text{Cd}_y\text{Mg}_{1-x-y}\text{Se}$

G. Comanescu, W. B. Wang, S. Gundry, B. Das, and R. R. Alfano^{a)}

Institute for Ultrafast Spectroscopy and Lasers, Department of Physics, City College and Graduate Center of the City University of New York, New York, New York 10031

M. N. Perez-Paz and M. C. Tamargo

Department of Chemistry, City College and Graduate Center of the City University of New York, New York, New York 10031

M. Muñoz

Physics Department, Virginia Commonwealth University, Richmond, Virginia 23284

I. Popov and L. L. Isaacs

Department of Chemical Engineering, City College and Graduate Center of the City University of New York, New York, New York 10031

(Received 26 October 2004; accepted 9 May 2005; published online 17 June 2005)

Time-resolved and steady-state photoluminescence, reflectivity, and absorption experiments were performed on CdSe quantum dots in $\text{Zn}_x\text{Cd}_y\text{Mg}_{1-x-y}\text{Se}$ barriers. Studies of the capture times of the photoexcited carriers into the quantum dots and of electron-hole recombination times inside the dots were performed. Photoluminescence rise time yielded capture times from 20 ps to 30 ps. All samples exhibit fast and slow photoluminescence decays, consistent with observing two independent but energetically overlapping decays. The faster relaxation times for the sample emitting in the blue range is 90 ps, whereas for the two samples emitting in the green it is 345 ps and 480 ps. The slower relaxation times for the sample emitting in blue is 310 ps, whereas for the samples emitting in green is 7.5 ns. These results are explained on the basis of the structural differences among the quantum-dot samples. © 2005 American Institute of Physics. [DOI: 10.1063/1.1947909]

Understanding the physics of self-assembled quantum dots (QDs) has advanced in various IV, III-V, and II-VI semiconductor systems.¹⁻⁴ Among them, II-VI semiconductors have significant advantages because of their large band gaps and their high exciton-binding energy.^{1,2,5} The $\text{Zn}_x\text{Cd}_y\text{Mg}_{1-x-y}\text{Se}$ quaternary alloys offer outstanding flexibility for simultaneously engineering both the bandgap and the lattice constant.⁶ The $\text{Zn}_x\text{Cd}_y\text{Mg}_{1-x-y}\text{Se}$ band gap can be adjusted from 2.1 eV to 3.6 eV while keeping the lattice constant matched to the InP substrate. Furthermore, the $\text{Zn}_x\text{Cd}_{1-x}\text{Se}/\text{Zn}_x\text{Cd}_y\text{Mg}_{1-x-y}\text{Se}$ system exhibits a large conduction-band offset to localize carriers.⁷ The molecular-beam epitaxy (MBE) growth of $\text{Zn}_x\text{Cd}_y\text{Mg}_{1-x-y}\text{Se}$, and the use of these alloys as barriers for quantum wells and QD structures presents a significant opportunity for new devices. Recently, CdSe QDs in $\text{Zn}_x\text{Cd}_y\text{Mg}_{1-x-y}\text{Se}$ showed bright luminescence throughout the visible range.⁸ The anticipated large CdSe/ $\text{Zn}_x\text{Cd}_y\text{Mg}_{1-x-y}\text{Se}$ conduction-band offset (up to 1.5 eV) highlights the potential of these materials to address new important technological directions, such as QD infrared (IR) photodetectors (QDIPs) with functionality extended into near-IR, and even up to the visible region; and intersubband cascade lasers with emission wavelength significantly shorter (i.e., 1.5 μm) than what is currently available in such devices.

To take full advantage of the CdSe/ $\text{Zn}_x\text{Cd}_y\text{Mg}_{1-x-y}\text{Se}$ QDs outstanding properties for use in optoelectronic emitters and detectors, a detailed and comprehensive understanding of the electronic and optical properties of these materials is

necessary. In this letter, this need is addressed by the measurements of optical transmission and reflectivity experiments from the ultraviolet to the IR, room and liquid-nitrogen temperature continuous wave photoluminescence (PL) experiments from 400 nm to 700 nm, and time-resolved PL experiments on three different CdSe/ $\text{Zn}_x\text{Cd}_y\text{Mg}_{1-x-y}\text{Se}$ QD samples.

The CdSe/ $\text{Zn}_x\text{Cd}_y\text{Mg}_{1-x-y}\text{Se}$ multiple QD (MQD) structures were grown with the same $\text{Zn}_x\text{Cd}_y\text{Mg}_{1-x-y}\text{Se}$ barrier and top layer growth conditions as those described in Ref. 8 (see Fig. 1). The QDs are formed by the self-assembly technique, during MBE growth. The only difference between the samples presented in Ref. 8 and the samples described in this letter is the active region. The size and, consequently, the PL

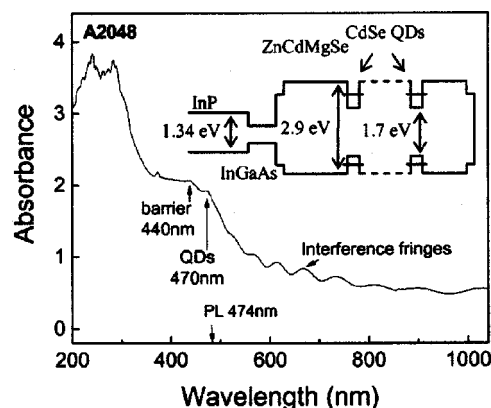


FIG. 1. Absorption spectrum of the Sample A2048 at 300 K. The position of the absorption peaks is indicated with the corresponding transitions. The inset shows the band structure of the QD samples.

^{a)}Electronic mail: alfano@scisun.sci.cuny.cuny.edu

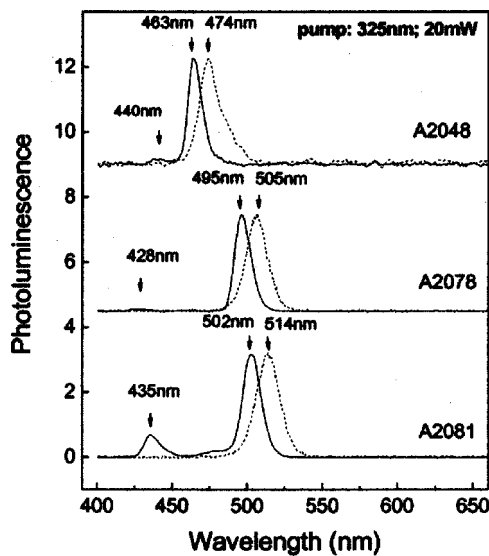


FIG. 2. PL spectra at 77 K (solid lines) and 300 K (dot lines) for Samples A2048, A2078, and A2081.

emission energy were controlled by the CdSe deposition time t_D (see Ref. 8). The MQD active regions of Samples A2078 and A2081 are composed of ten stacked CdSe QDs layers with the same $t_D=13$ s, 2.5 monolayers (MLs), corresponding to green emission, separated by $\text{Zn}_x\text{Cd}_y\text{Mg}_{1-x-y}\text{Se}$ spacers with different thickness, 32.5 nm for A2078 and 5.2 nm for A2081. The sample A2048 is a MQD structure that consists of nine QD layers of stacked QDs with a 130 nm ZnCd-MgSe spacers: From the top to the bottom, six QD layers with $t_D=6$ s (1.2 ML), two QDs layers with $t_D=18$ s (3.6 ML), and one layer of QDs with $t_D=36$ s (7.2 ML).

In Ref. 8, a three-dimensional atomic force microscopy (AFM) image of an uncapped single layer of CdSe QDs on a $\text{Zn}_x\text{Cd}_y\text{Mg}_{1-x-y}\text{Se}$ barrier with a $t_D=10$ s (2 ML) is given. The samples for AFM measurement were removed from the chamber immediately following the CdSe deposition (without the quaternary top and cap layers). To slow down a possible ripening effect and the formation of oxides⁵ the samples were immediately immersed in liquid nitrogen after the growth and kept in this condition until the moment of taking the surface topography by AFM under ambient conditions. Although the AFM image gives an idea of the QD shape and size distribution in our samples, the samples that were studied in this work do not have the same size as the sample in the AFM image, since different deposition times were used, and in general, even for similar deposition times, capped and uncapped QDs exhibit different sizes.⁸

The study of the interband QDs absorption for CdSe/ $\text{Zn}_x\text{Cd}_y\text{Mg}_{1-x-y}\text{Se}$ MQD samples grown on InP substrates is impaired by the InP substrate (the InP band gap is lower than that of the interband QDs absorption energy). Thus, we removed the InP substrate from the CdSe/ $\text{Zn}_x\text{Cd}_y\text{Mg}_{1-x-y}\text{Se}$ QDs active structure by selective chemical etching.⁹ We have performed optical transmission and reflectivity measurements on all three QD samples for the spectral range of 180 nm to 3200 nm. The absorption spectrum at room temperature of Sample A2048 is shown in Fig. 1. The feature at 470 nm corresponds to the interband QDs absorption whereas the one at 440 nm corresponds to the band gap of the $\text{Zn}_x\text{Cd}_y\text{Mg}_{1-x-y}\text{Se}$ barrier. For Sample A2078, the features corresponding to QDs interband absorp-

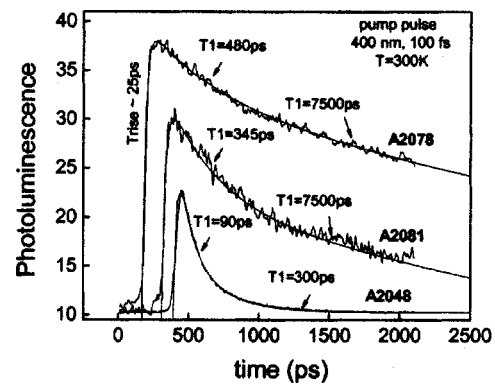


FIG. 3. Time-resolved PL spectra at 300 K and fit lines for Samples A2078, A2081, and A2048.

tion and $\text{Zn}_x\text{Cd}_y\text{Mg}_{1-x-y}\text{Se}$ bulk absorption are observed at about 497 nm and 440 nm, respectively. Sample A2081 absorption spectrum is similar to the one of A2078. Reflectivity measurements between 300 nm and 800 nm, at 300 K have been performed on all samples. Reflectivity spectra on all samples show clearly the $\text{Zn}_x\text{Cd}_y\text{Mg}_{1-x-y}\text{Se}$ band-gap signature at about 440 nm.

PL spectra at 300 K and 77 K have been measured on all QD samples, as shown in Fig. 2. For PL measurements a He-Cd laser was used with an excitation intensity of 20 mW. The peaks corresponding to interband transitions in the QDs and the bulk $\text{Zn}_x\text{Cd}_y\text{Mg}_{1-x-y}\text{Se}$ barriers are observed. Sample A2048 at 77 K shows a strong luminescence peak at 463 nm corresponding to the QDs interband transitions and a weak peak at 440 nm from the $\text{Zn}_x\text{Cd}_y\text{Mg}_{1-x-y}\text{Se}$ barrier. At 300 K, the QD peak shifts to 474 nm and the barrier peak disappears. We attribute this PL peak to the top QDs ($t_D=6$, s 1.2 ML). No other peaks could be seen from the other QDs, the two QD layers with $t_D=18$ s (3.6 ML) and the one with $t_D=36$ s (7.2 ML), in this sample. The fact that no emission from the deeper QDs is observed is probably due to the larger number of blue QD layers (six layers with $t_D=6$ s), with respect to the other two types of QDs layers, as well as to the large $\text{Zn}_x\text{Cd}_y\text{Mg}_{1-x-y}\text{Se}$ spacer thickness, which makes the active region in this sample very thick; thus, very little light is likely to be penetrating to the deeper QDs. Samples A2078 and A2081 show strong emission at 505 nm and 514 nm, respectively, at 300 K. The difference between the PL peak positions of these two green samples could be due to the slight shift in the barrier composition (more magnesium in the barrier of Sample A2078). The QDs emission of these samples is slightly blueshifted to 495 nm and 502 nm, respectively, for PL collected at 77 K. Sample A2081 shows a substantially stronger barrier emission than Sample A2078. This can be explained when we consider the very different total thickness of the QD active region (spacers and QDs) for the two samples, $10 \times 5.2 \text{ nm} = 52 \text{ nm}$ for A2081 and $10 \times 32 \text{ nm} = 320 \text{ nm}$ for A2078. Thus, electrons photoexcited into the $\text{Zn}_x\text{Cd}_y\text{Mg}_{1-x-y}\text{Se}$ material surrounding the QDs ($\sim 700 \text{ nm}$) spend more time in the active region for the A2078 sample than for the A2081 sample because the active region in A2078 is much thicker than in A2081. As a result, a larger percentage of the photoexcited electrons recombine in the bulk $\text{Zn}_x\text{Cd}_y\text{Mg}_{1-x-y}\text{Se}$ for Sample A2081 than for Sample A2078. The fact that the 300 K PL for all samples does not exhibit features corresponding to $\text{Zn}_x\text{Cd}_y\text{Mg}_{1-x-y}\text{Se}$ bulk emission, while the 77 K PL for the same samples ex-

TABLE I. PL decay times, rise times, and monitored PL peak for all samples.

| Sample | Fast decay time (ps) | Slow decay time (ps) | Rise time (ps) | PL at 300 K (nm) | QD layers interspacing (nm) |
|--------|----------------------|----------------------|----------------|------------------|-----------------------------|
| A2048 | 90 | 310 | ~30 | 474 | 130 |
| A2078 | 480 | 7500 | ~22 | 505 | 32.5 |
| A2081 | 345 | 7500 | ~25 | 514 | 5.2 |

hibit $\text{Zn}_x\text{Cd}_y\text{Mg}_{1-x-y}\text{Se}$ bulk emission, indicates that the carriers photoexcited into the $\text{Zn}_x\text{Cd}_y\text{Mg}_{1-x-y}\text{Se}$ are captured into the QDs faster at higher temperatures. This is expected because the electron kinetic energy is higher at 300 K than at 77 K. The peaks in the PL at 300 K in all samples are Stokes shifted about 25 meV toward lower energy with respect to the corresponding absorption peak. These Stokes shifts are consistent with other studies on QDs.¹⁰

Time-resolved PL measurements were performed at 300 K for all three samples. The electrons and holes photoexcited (400 nm, 100 fs pulse) into the $\text{Zn}_x\text{Cd}_y\text{Mg}_{1-x-y}\text{Se}$ relax into the QDs subbands, recombine and emit PL photons. Figure 3 shows the PL intensity as function of time for all the samples. The rise time gives information about the capture of electrons and holes into the QDs, whereas the decay time reflects the electron-hole recombination inside the QDs. All three samples exhibit a fast and a slow PL decay component. The time-resolved traces in Fig. 3 are fit to a sum of two exponential decays and one exponential rise. Table I summarizes the decay times, the rise time, and the corresponding monitored PL peaks for each sample. The existence of multiple exponential decays is consistent with observing multiple independent but energetically overlapping decays. Similar biexponential decays in the PL of CdSe QDs have been observed in other experiments.^{10–13} The biexponential decays can be explained either by the existence of two independent recombination channels inside the same quantum dots^{10–13} or, in the case of self-assembled QDs grown by MBE, by the coexistence of two types of QDs, of slightly different shapes, in the same sample.¹⁴ Further work is necessary to understand the mechanism of biexponential decay.

All of the samples studied exhibit strong PL even at room temperature, which indicates that they have good structural quality. The fact that both recombination processes in Sample A2048 are substantially faster (90 ps, 310 ps) than the ones for Samples A2078 and A2081 (400 ps, 7.5 ns) suggests that the recombination processes are inherently faster in smaller QDs (the QDs emitting in blue are smaller than the ones emitting in green) because of large influence of the QD surface on the electronic states. It is interesting to compare the PL and the time-resolved PL from these two samples, because the two samples have the same layer composition but different QD layer interspacing (Sample A2078—32.5 nm, and Sample A2081—5.2 nm). The slow relaxation process is almost the same for both samples, ~7.5 ns, whereas the fast relaxation process is substantially faster for the sample with smaller interspacing between QD layers than that for the sample with larger interspacing be-

tween QD layers. These data suggest that the fast relaxation process may be influenced by the perturbation between adjacent QD layers, whereas the slow relaxation process is not influenced by factors outside the QDs.

In summary, steady-state and time-resolved PL and absorption experiments have been performed for CdSe/ $\text{Zn}_x\text{Cd}_y\text{Mg}_{1-x-y}\text{Se}$ MQDs samples. All samples exhibit a fast and a slow photoluminescence decay component. The capture time of the photoexcited carriers from barriers into the QDs and recombination times inside the dots have been evaluated for the first time for CdSe QDs with $\text{Zn}_x\text{Cd}_y\text{Mg}_{1-x-y}\text{Se}$ barriers (see Table I). The existence of two exponential decays is consistent with observing two independent but energetically overlapping decays. The substantially faster relaxation in the samples with smaller QDs is attributed to the larger perturbative influence that the surface of the QDs has on the electronic states of the QDs. The strong PL emission throughout the visible range, and the rather long 7.5 ns QD interband relaxation shows that the CdSe QDs with 2.8 eV $\text{Zn}_x\text{Cd}_y\text{Mg}_{1-x-y}\text{Se}$ barriers are suitable for optoelectronic devices such as QD lasers and QD visible and IR photodetectors. The fact that $\text{Zn}_x\text{Cd}_y\text{Mg}_{1-x-y}\text{Se}$ alloys, with 2.8 eV band gap, have been successfully used as barrier materials for CdSe QDs, with large conduction-band offsets, allows us to explore several new important directions, such as QDIPs with functionality that extends into the near-IR, up to the visible region; and intersubband quantum cascade lasers with emission wavelength significantly shorter (i.e., 1.5 μm) than what is currently available in such devices.

This work was supported in part by the Department of Defense—Grant No. W911NF-04-1-0023, and by National Science Foundation—Grant No. ECS0217646.

¹*II-VI Semiconductor Materials and their Applications*, edited by Maria Tamargo (Taylor and Francis, New York, 2002), Vol. 12.

²M. C. Tamargo, W. Lin, S. P. Guo, Y. Guo, Y. Luo, and Y. C. Chen, *Cryst. Growth* **214**, 1058 (2000).

³K. Shum, W. B. Wang, R. R. Alfano, and K. M. Jones, *Phys. Rev. Lett.* **68**, 3904 (1992).

⁴Y. Luo, S. P. Guo, O. Maksimov, M. C. Tamargo, V. Asnin, F. H. Pollak, and Y. C. Chen, *Appl. Phys. Lett.* **77**, 4259 (2000).

⁵J. E. Bowen Katari, V. L. Colvin, and A. P. Alivastatos, *J. Phys. Chem.* **98**, 4109 (1994).

⁶L. Zeng, B. X. Yang, A. Cavus, W. Lin, Y. Y. Luo, M. C. Tamargo, Y. Guo, and Y. C. Chen, *Appl. Phys. Lett.* **72**, 3136 (1998).

⁷M. Muñoz, H. Lu, X. Zhou, M. C. Tamargo, and F. H. Pollak, *Appl. Phys. Lett.* **83**, 1995 (2003).

⁸M. N. Perez-Paz, X. Zhou, M. Munoz, H. Lu, M. Sohel, M. C. Tamargo, F. Jean-Mary, D. L. Akins, *Appl. Phys. Lett.* **85**, 6395 (2004).

⁹J. R. Lothian, J. M. Kuo, F. Ren, and S. J. Pearton, *J. Electron. Mater.* **21-4** p. L100 (1992).

¹⁰A. Javier, D. Magana, T. Jenings, and G. F. Strouse, *Appl. Phys. Lett.* **83**, 1423 (2003).

¹¹G. Schlagel, J. Bohnenberger, I. Potapova, and A. Mews, *Phys. Rev. Lett.* **88**, 137401-1 (2002).

¹²L. M. Robinson, H. Rho, J. C. Kim, H. E. Jackson, L. M. Smith, S. Lee, M. Dobrowolska, and J. K. Furdyna, *Phys. Rev. Lett.* **83**, 2797 (1999).

¹³D. V. Regelman, E. Dekel, D. Gershoni, E. Ehrenfreund, A. J. Williamson, J. Shumway, A. Zunger, W. V. Schoenfeld, and P. M. Petroff, *Phys. Rev. B* **64**, 165301-1 (2001).

¹⁴M. Strassburg, T. Deniozou, A. Hoffmann, R. Heitz, U. W. Pohl, D. Bimberg, D. Litvinov, A. Rosenauer, D. Gerthsen, S. Schwedhelm, K. Lischka, and D. Shikora, *Appl. Phys. Lett.* **76**, 685 (2000).